

Reconstruction of the vertical profile of mean atmospheric transmittance from data of optical observations of cosmic rays

M.N. D'yakonov, S.P. Knurenko, V.A. Kolosov, and I.E. Sleptsov

Institute for Space-Physical Research and Aeronomy, Yakutsk

Received July 17, 1998

We propose a method to obtain information about the integral atmospheric transparency from measurements of a spatial distribution of Cherenkov radiation $Q(R)$ from extended atmospheric showers of ultrahigh energy ($E_0 \geq 10^{17}$ eV). From measurement data on $Q(R)$, vertical profiles of mean atmospheric transmittance are reconstructed for three grades of weather conditions: with very high, high, and normal transparency. The results are used to estimate the effective atmospheric transparency for every case. This allowed us to refine some characteristics of the extended atmospheric showers of ultrahigh energy.

Introduction

Cosmic rays of ultrahigh energy, interacting with the atomic nuclei in air, generate a cascade of secondary particles, which is called the extensive air shower (EASh). Such a shower is accompanied by high-power coherent electromagnetic radiation, the most efficient among which is Cherenkov radiation generated by relativistic particles of EASh in the optical wavelength region.

The idea of the proposed method is that the value of radiation extinction along a propagation path can be estimated from the power of a radiation source at a given height by measuring the radiation intensity at the level of observations. Earlier, in Refs. 1 and 2, we have determined the atmospheric transparency from the relative change in the integral frequency of Cherenkov radiation "flashes" for EASh with the energy as high as $10^{15} - 10^{16}$ eV. These flashes corresponded to the mean height of the radiation source ranging from 5.0 to 6.5 km. In this paper we propose a new method to estimate the atmospheric transmittance for EASh with the energy about 10^{18} eV, the radiation source of which is located at the height about 3.5 km. This method is based on recording the density of Cherenkov radiation flux from EASh at different distance from a EASh axis. Since the detector of Cherenkov radiation used (FEU-49B) is sensitive in the wavelength range from $\lambda_1 = 360$ to $\lambda_2 = 800$ nm, it is worth considering the integral transparency of the atmosphere. In this case we should keep in mind that the detector's sensitivity is maximum at $\lambda = 420$ nm and that the spectral power of the radiation source falls off with increasing wavelength as λ^{-2} .

To analyze the data on the ultrahigh-power cosmic rays, it is very important to state the problem of reconstruction of the vertical profile of the atmospheric transmittance correctly and to solve it adequately. The data for our analysis have been obtained with an EASh setup in Yakutsk. When considering the problem in detail, the ill-posed problem of the type of the

Fredholm integral equation of the first kind arises. To solve it, one has to use modern methods for solution of the inverse problems. Taking into account the conditions of our experiments, we have selected, from the regularizing algorithms available, the adaptive method.³ In the mathematical statement of the problem and *a priori* information available, this method suits our problem best of all.

Initial equation

Detectors usually measure the flux density $Q(R)$ of Cherenkov radiation at a fixed distance R from the axis of a shower. A set of such measurement points represents the spatial distribution of radiation at the level of observations. The power of a radiation source at the altitude z in the atmosphere depends on the product of the total number of particles $N(z)$ by the light yield function $g(R, z)$. Here the R dependence of $g(R, z)$ reflects the fact of angular distribution of these particles and the probability that radiation from them comes to this distance. The initial equation can be written in the form

$$Q(R) = \int_0^{\infty} A(R, z) T(z) dz. \quad (1)$$

Here $T(z)$ is the transmittance of the atmosphere from the altitude z to the level of observations, and the number of photons emitted on a unit path length is

$$A(R, z) = g(R, z) N(z) \rho(z), \quad (2)$$

where $\rho(z)$ is the air density at the altitude z .

The function $g(R, z)$ depends on the power spectrum of emitting particles and the energy threshold for Cherenkov effect. When an inverse problem on the unknown $T(z)$ is stated, Eq. (1) takes the form of the Fredholm integral equation of the first kind, which falls in the category of ill-posed inverse problems. Such problems are usually solved by introducing some *a priori* information about a solution sought, based on physical grounds of the problem.

Method of solution

Applying Chebyshev quadrature formula, represent Eq. (1) as a system of linear algebraic equations:

$$\sum_{j=1}^m A_{ij} T_j = Q_i, \quad i = 1, \dots, n; \quad j = 1, \dots, m, \quad (3)$$

where n is the total number of detectors responded; m is the number of points at different altitudes in the atmosphere, at which the atmospheric transmittance is being reconstructed.

The set of equations (3) has been solved using the adaptive method for solution of inverse problems. This method uses the vectors of initial approximations of the unknown $T_j^{(0)}$ and their certainties σ_{T_j} as an *a priori* information. Having substituted $T_j^{(0)}$ into the i th equation of the set (3), we obtain the prognostic value of \bar{Q}_i . The difference $\Delta Q_i = Q_i - \bar{Q}_i$ is referred to as the discrepancy. It can be presented as a sum:

$$\Delta Q_i = \sum_{j=0}^m u_j, \quad (4)$$

where it is meant that $u_0 = \xi_i$, and ξ_i are measurement errors.

All terms are assumed independent random values distributed by the normal law. Then the joint probability density in the $(m + 1)$ -dimensional space has the form

$$\mu(u_0, \dots, u_m) = \prod_{j=0}^m 1/(\sqrt{2\pi}\sigma_{u_j}) \exp(-u_j^2/2\sigma_{u_j}^2), \quad (5)$$

where

$$\sigma_{u_j}^2 = (A_{ij} \sigma_{T_j})^2, \quad \sigma_{u_0}^2 = \sigma_{\bar{Q}_i}^2; \quad u_0 = (\Delta Q_i - \sum_{j=1}^m u_j); \quad (6)$$

$\sigma_{\bar{Q}_i}$ is the rms measurement error.

The values of u_j are chosen so that the probability density is maximal. This can be achieved when the goal function

$$v(u_1, \dots, u_m) = u_0^2/\sigma_{\bar{Q}_i}^2 + \sum_{j=1}^m u_j^2/\sigma_{u_j}^2 \quad (7)$$

takes its minimum.

It is easy to see that the goal function is similar to the Tikhonov minimizing functional. If it is accepted that $\sigma_{\bar{Q}_i} = \sigma_Q$, $\sigma_{u_j} = \sigma_u$, and $\alpha = \sigma_Q^2/\sigma_u^2$, then we have

$$\min v(u_1, \dots, u_m) = (\Delta Q_i - \sum_{j=1}^m u_j)^2 + \alpha \sum_{j=1}^m u_j^2, \quad (8)$$

what exactly corresponds to the Tikhonov regularizing functional. Having differentiated Eq. (8) with respect to every unknown parameter, we obtain a set of n equations for m unknowns. This set has the following solution:

$$u_j = \Delta Q_i [\sigma_{u_j}^2 / (\sigma_{\bar{Q}_i}^2 + \sum_{j=1}^m \sigma_{u_j}^2)]. \quad (9)$$

Upon designating the second cofactor in Eq. (9) as β_{ij} and introducing the number of the next refining step k , we obtain the recursion expression

$$T_j^{(k+1)} = T_j^{(k)} + \Delta Q_i^{(k+1)} \beta_{ij} / A_{ij}. \quad (10)$$

As the number of iteration increases, the rms error of the obtained solution decreases:

$$(\sigma_{u_j}^2)^{k+1} = (\sigma_{u_j}^2)^k (1 - \beta_{ij}). \quad (11)$$

This follows from the fact that the parameter β_{ij} varies from 0 to 1, and the rms error decreases, thus leading to the needed refinement of the solution sought.

Experimental data

The EASH complex in Yakutsk has a network of observation stations distributed over the area of $\sim 11 \text{ km}^2$ separated by a distance of 500 and 1000 m from each other.⁴ Every station has a detector, which detects Cherenkov radiation from EASH in nighttime under clear-sky conditions without Moon.

It follows from calculations made in Ref. 5, that scattering and absorption of photons in the atmosphere, as Cherenkov radiation flux propagates from the source at an altitude z_m to the observation level z_0 , have different effect on the value of the flux density of Cherenkov radiation from EASH at different distance R from the shower axis. Therefore, measuring Cherenkov radiation fluxes at certain distances R from the shower axis under the same atmospheric conditions, we can estimate the atmospheric transmittance from the shape of the spatial distribution of Cherenkov radiation. Toward this end, EASHs have been selected using a shower parameter, which is independent of the atmospheric conditions, as a selection criterion. Such a parameter is the density of a flux of charged particles at a distance $R = 300 \text{ m}$ from the shower axis. The parameter $\rho(300)$ depends on the primary shower energy; thus, showers were grouped by the altitude of the radiation source. The radiation source was assumed to be a point source in our case, and the radiation flux was considered to be parallel. Besides, the showers were classified according to the visual evaluation of the atmospheric transparency, divided in the groups of 5, 4, and 3 visibility classes (Ref. 6). The transparency of 5, at which the Milky Way is clearly seen and individual stars can be distinguished by eye against the sky background, is "very highB" in meteorological terms. At the transparency of 4 ("highB"), the Milky Way is clearly seen all over the sky. At the transparency of 3 ("normalB"), the Milky Way is not seen, only some bright stars and constellations can be observed by eye. According to the above said, three classes of showers were formed. In all the three classes, the mean value of $\rho(300)$ was equal to 14.6 particles per 1 m^2 , what corresponds to the initial energy $e_0 = 10^{18} \text{ eV}$ and the

intensity of cosmic rays $I = 7 \cdot 10^{-12} \text{ m}^{-2} \cdot \text{s}^{-1} \cdot \text{sr}^{-1}$ according to the power spectrum measured in Ref. 7. Figure 1 shows the spatial distribution of the flux density of Cherenkov radiation from EASh $Q(R)$, corresponding to these three classes of showers at different atmospheric transparency. In Fig. 1 one can see a slight difference, in the absolute value, between $Q(R)$ obtained for the transparency of 5 and 4 classes and the marked difference between the curves corresponding to the transparency of 5th and 3rd classes. The shape of function $Q(R)$ has also changed a little bit. For example, for the transparency of the 5th class, the slope of $Q(R)$, when described by the exponential function $Q(R) \propto R^{-n}$ in the range $100 \leq R \leq 500 \text{ m}$ from the shower axis, corresponds to $n = 2.05 \pm 0.13$. For the transparency of the 4th class, $n = 2.09 \pm 0.11$; for the transparency of the 3rd class, $n = 2.32 \pm 0.08$. Thus, the change in the atmospheric transmittance can result in a redistribution of radiation over distance and, consequently, in a change of the $Q(R)$ shape (Table 1). These data were used to reconstruct the vertical profile of the atmospheric transmittance under different optical conditions in the atmosphere.

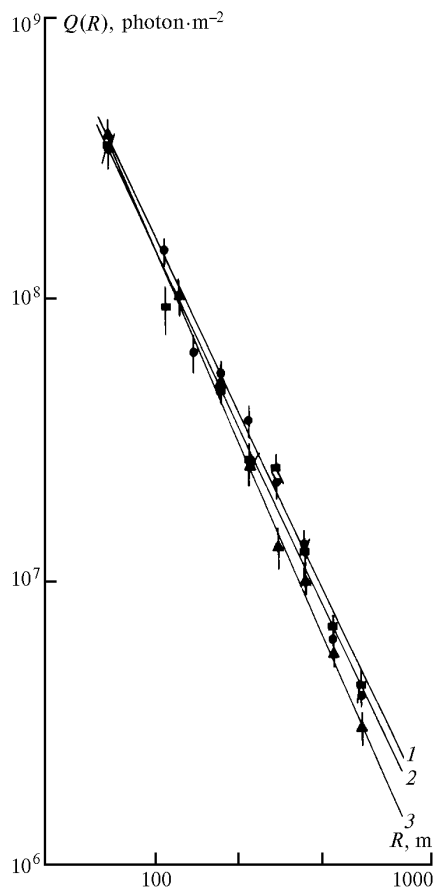


Fig. 1. Spatial distribution of Cherenkov radiation from EASh under different weather conditions: atmospheric transparency of the 5th class (curve 1), 4th class (curve 2), and the 3rd one (curve 3).

Table 1. Values of $Q(R)$ corresponding to the approximation of experimental points by the exponential function for the three classes of visual evaluation of the atmospheric transparency.

$R, \text{ m}$	Transparency of 5	Transparency of 4	Transparency of 3
50	$7.40 \cdot 10^8$	$6.60 \cdot 10^8$	$7.56 \cdot 10^8$
63	$4.80 \cdot 10^8$	$4.44 \cdot 10^8$	$4.70 \cdot 10^8$
79	$2.84 \cdot 10^8$	$2.59 \cdot 10^8$	$2.74 \cdot 10^8$
100	$1.71 \cdot 10^8$	$1.54 \cdot 10^8$	$1.54 \cdot 10^8$
126	$1.08 \cdot 10^8$	$9.34 \cdot 10^7$	$9.01 \cdot 10^7$
159	$6.31 \cdot 10^7$	$5.63 \cdot 10^7$	$5.06 \cdot 10^7$
200	$4.01 \cdot 10^7$	$3.54 \cdot 10^7$	$3.06 \cdot 10^7$
252	$2.46 \cdot 10^7$	$2.21 \cdot 10^7$	$1.85 \cdot 10^7$
317	$1.57 \cdot 10^7$	$1.38 \cdot 10^7$	$1.12 \cdot 10^7$
400	$9.67 \cdot 10^6$	$8.23 \cdot 10^6$	$6.51 \cdot 10^6$
504	$5.84 \cdot 10^6$	$5.06 \cdot 10^6$	$3.71 \cdot 10^6$
634	$3.66 \cdot 10^6$	$3.16 \cdot 10^6$	$2.24 \cdot 10^6$
800	$2.37 \cdot 10^6$	$2.05 \cdot 10^6$	$1.41 \cdot 10^6$

Results

The problem presented by Eq. (1) is solved using the initial approximation $T_j^{(0)} = \text{const}$ (the most neutral assumption on the sought solution) and vectors of certainties σ_{T_j} presented in Table 2. Besides, in Eq. (3) the error in the right-hand side can be written as

$$\sigma_{Q_i}^2 = \{0.04 + n^2 (\Delta R/R)^2\} Q_i^2, \quad (12)$$

where ΔR is the error in determination of the shower axis; the factor equal to 0.04 is due to the absolute calibration of radiation detectors, and n are the above-determined exponents at the exponential approximation of $Q(R)$.

The results obtained are shown in Fig. 2 as a vertical profile of the atmospheric transmittance and the generalized form of the results is given in Table 2.

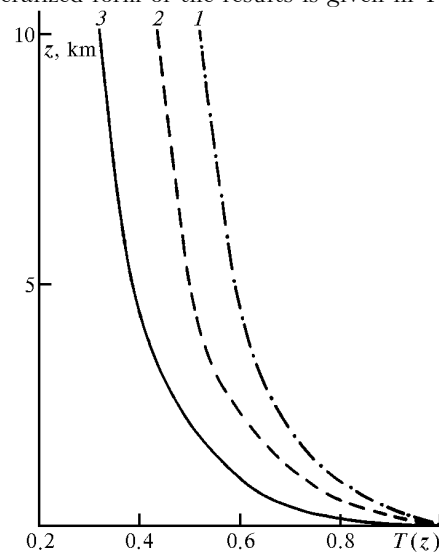


Fig. 2. Vertical profiles of the mean atmospheric transmittance under different atmospheric conditions. The designations are the same as in Fig. 1.

Table 2.

Transparency	σ_{T_j}, T_j	z, m					
		500	2150	3200	5220	7820	10100
5	σ_{T_j}	0.50	0.33	0.31	0.37	0.72	1.87
5	T_j	0.87 ± 0.0	0.69 ± 0.0	0.64 ± 0.0	0.59 ± 0.0	0.55 ± 0.0	0.53 ± 0.1
4	σ_{T_j}	0.47	0.28	0.26	0.30	0.50	1.55
4	T_j	0.80 ± 0.1	0.62 ± 0.0	0.55 ± 0.0	0.50 ± 0.0	0.47 ± 0.0	0.45 ± 0.1
3	σ_{T_j}	0.25	0.32	0.34	0.44	1.13	5.75
3	T_j	0.67 ± 0.1	0.50 ± 0.0	0.44 ± 0.0	0.39 ± 0.0	0.35 ± 0.0	0.33 ± 0.1

As seen from Fig. 2 the curves corresponding to the atmospheric transmission functions, under different conditions, differ markedly both in the absolute value and in the shape of the vertical profile of the atmospheric transmittance. From comparing T_j with the altitude behavior of the theoretically calculated atmospheric transmittance due to molecular scattering, we can find that the contribution from the aerosol component is greatest at altitudes of 2 to 3 km. The curvature of the functions plotted allows us to conclude that the contribution from the aerosol component is most significant at the atmospheric transparency evaluated visually as the class 3.

In order to estimate the integral atmospheric transparency, we should find the total flux $\Phi(e_0, \lambda)$ of Cherenkov radiation from EASH by the following expression:

$$\Phi_i(e_0, \lambda) = 2\pi \int_0^\infty Q_i(E_0, R, \lambda) R dR, \quad (13)$$

where the subscripts $i = 1, \dots, 3$ correspond to visual evaluation of the atmospheric transparency; e_0 is the energy of the initially incident cosmic particle, which has initiated the shower at the atmospheric boundary; λ is the wavelength of radiation emitted by the secondary shower particles. With the experimentally measured total radiation flux Φ_{exp} , we can find the energy E_i emitted by shower particles in the atmosphere:

$$E_i = k(z_m, T_{\Delta\lambda}) \Phi_{exp}, \quad (14)$$

where k is the coefficient, which depends directly on the absolute transparency of the atmosphere and the energy of the primary particle, parameterized through the radiation source altitude z_m .

Actually, the energy E_i makes up ~80% of the primary particle energy E_0 . Given the radiation propagates through the atmosphere without loss, the total radiation flux $\Phi_0(e_0, \lambda)$ at the observation level can be calculated by Eq. (13), where $Q_0(e_0, R, \lambda)$ is found from Eq. (1) at $T(z) \equiv 1$. To analyze the measured data on EASH characteristics, we need the effective atmospheric transparency,⁶ rather than the spectral one. The former can be found as

$$T_{i,\Delta\lambda}(E_0) = \frac{\int_{\lambda_1}^{\lambda_2} \Phi_i(E_0, \lambda) S(\lambda) g(\lambda) d\lambda}{\int_{\lambda_1}^{\lambda_2} \Phi_0(E_0, \lambda) S(\lambda) g(\lambda) d\lambda}, \quad (15)$$

where $S(\lambda)$ is the spectrum of an actual radiation source; $g(\lambda)$ is the instrumental function depending on the spectral characteristic of the FEU-49B photomultiplier.

The values of $T_i(E_0)$ obtained in such a way are $T_5 = 0.67$, $T_4 = 0.6$, and $T_3 = 0.49$ at the atmospheric transparency evaluated visually as the class 5, 4, and 3, respectively. It should be emphasized that the value $T_5 = 0.67$ corresponds to the conditions of very high transparency. Under such atmospheric conditions, the extinction of the flux of Cherenkov radiation from EASH is minimal and close to the Rayleigh scattering profile. For the transparency of the 4th and 3rd class, as follows from their comparison with the case of the transparency of the 5th class, there appear significant differences in the radiation fluxes. For example, the difference between the results obtained for the transparency of the 5th and 4th class is 10%, while reaching 30% between the results obtained at the transparency corresponding to the 5th and 3rd classes. This leads to deformation of the shape of the spatial distribution function of Cherenkov light and thus to distortions in all information that follows as well: shower energy, characteristics of longitudinal evolution of showers, and others.

Conclusion

The obtained results on reconstruction of the altitude profile of the atmospheric transmittance allow the following conclusions to be drawn.

1. Since the atmospheric transparency evaluated for the 5th class conditions is 7% lower than its value accepted earlier,² the initial energy calculated with the use of Eq. (14) should be corrected for this value.

2. The spatial distribution of Cherenkov radiation from EASH is also used to reconstruct the longitudinal

evolution of showers in the atmosphere.⁸ Therefore, to reconstruct it correctly, the vertical profile of the atmospheric transmittance must be known. The data we have obtained allowed the estimation to be made of the correction factors for u_{\max} – the depth of the EASh evolution maximum. In particular, for the transparency of the 4th class, it is (12 ± 4) g/cm²; while for the transparency of the 3rd class, it is (27 ± 6) g/cm².

According to these corrections, the earlier obtained values of the depth of the shower evolution maximum⁹ should be refined.

The reconstructed profiles of the atmospheric transmission function can also be used by other researchers in studying the phenomena of EASh both experimentally and theoretically.

3. Besides, with known vertical profiles of the atmospheric transmittance at atmospheric transparency of the 3rd and 4th class, we can extend the statistics of analyzed events by, on average, 30–40% (earlier it included only the data corresponding to the transparency of the 5th class).

References

1. F.F. Lishchenyuk, Inventor's Certificate No. 519768, 1976.
2. M.N. D'yakonov, S.P. Knurenko, V.A. Kolosov, and I.E. Sleptsov, *Atm. Opt.* **4**, No. 8, 612–615 (1991).
3. V.A. Kochnev, in: *Use of Computers in Control Problems* (Krasnoyarsk, 1985), pp. 62–71.
4. V.P. Artamonov, B.N. Afanas'ev, A.V. Glushkov, et al., *Izv. Ros. Akad. Nauk, Ser. Fiz.* **58**, No. 12, 92–97 (1994).
5. M.N. D'yakonov, V.A. Kolosov, D.D. Krasil'nikov, et al., *Izv. Akad. Nauk SSSR, Ser. Fiz.* **39**, No. 6, 1243–1251 (1975).
6. G.P. Gushchin, *Methods, Instrumentation, and Results of Spectral Atmospheric Transparency Measurements* (Gidrometeoizdat, Leningrad, 1988), 196 pp.
7. C. Aguirre, R. Anda, A. Trepp, et al., in: *Proc. 16th ICRC, Kyoto, Japan* (1979), Vol. 8, pp. 107–110.
8. M.N. Dyakonov, A.A. Ivanov, S.P. Knurenko, et al., in: *Proc. 23th ICRC, Calgary* (1993), Vol. 4, p. 303.
9. M.N. D'yakonov, A.A. Ivanov, S.P. Knurenko, et al., in: *Proceedings of Yakutsk Affiliate of the Siberian Branch of the USSR Academy of Sciences* (1985), pp. 15–19.